

Semi-analytic study on the conductance of a lengthy armchair honeycomb nanoribbon including vacancies, defects, or impurities

Fateme Nadri, Mohammad Mardaani, Hassan Rabani

Citation: Chin. Phys. B . 2019, 28(1): 017202. **doi:** 10.1088/1674-1056/28/1/017202
Journal homepage: http://cpb.iphy.ac.cn; http://iopscience.iop.org/cpb

What follows is a list of articles you may be interested in

Electrical controllable spin valves in a zigzag silicene nanoribbon ferromagnetic junction

Lin Zhang(张林)

Chin. Phys. B . 2018, 27(6): 067203. **doi:** 10.1088/1674-1056/27/6/067203

Transport properties of zigzag graphene nanoribbons adsorbed with single iron atom

Yang Yu-E, Xiao Yang, Yan Xiao-Hong, Dai Chang-Jie

Chin. Phys. B . 2015, 24(11): 117204. **doi:** 10.1088/1674-1056/24/11/117204

Adiabatic quantum pump in a zigzag graphene nanoribbon junction

Zhang Lin

Chin. Phys. B . 2015, 24(11): 117202. **doi:** 10.1088/1674-1056/24/11/117202

Valley selection rule in a Y-shaped zigzag graphene nanoribbon junction

Zhang Lin, Wang Jun

Chin. Phys. B . 2014, 23(8): 087202. **doi:** 10.1088/1674-1056/23/8/087202

Spin-polarized transport in graphene nanoribbon superlattices

Yu Xin-Xin, Xie Yue-E, Yang Tao, Chen Yuan-Ping

Chin. Phys. B . 2012, 21(10): 107202. **doi:** 10.1088/1674-1056/21/10/107202

Semi-analytic study on the conductance of a lengthy armchair honeycomb nanoribbon including vacancies, defects, or impurities

Fateme Nadri[1], Mohammad Mardaani[1,2,†], and Hassan Rabani[1,2]

[1] *Department of Physics, Faculty of Science, Shahrekord University, P. O. Box* 115 *Shahrekord, Iran*
[2] *Nanotechnology Research Center, Shahrekord University,* 8818634141 *Shahrekord, Iran*

(Received 9 September 2018; revised manuscript received 6 November 2018; published online 25 December 2018)

We present a semi-analytic method to study the electronic conductance of a lengthy armchair honeycomb nanoribbon in the presence of vacancies, defects, or impurities located at a small part of it. For this purpose, we employ the Green's function technique within the nearest neighbor tight-binding approach. We first convert the Hamiltonian of an ideal semi-infinite nanoribbon to the Hamiltonian of some independent polyacetylene-like chains. Then, we derive an exact formula for the self-energy of the perturbed part due to the existence of ideal parts. The method gives a fully analytical formalism for some cases such as an infinite ideal nanoribbon and the one including linear symmetric defects. We calculate the transmission coefficient for some different configurations of a nanoribbon with special width including a vacancy, edge geometrical defects, and two electrical impurities.

Keywords: nanoribbon, conductance, vacancy, impurity, Green's function

PACS: 72.80.Vp, 72.10.–d, 73.23.–b, 78.67.Uh **DOI:** 10.1088/1674-1056/28/1/017202

1. Introduction

Graphene nanoribbons (GNRs), which are the bases for constructing carbon nanostructures, are the most famous honeycomb networks.[1,2] In recent years, they have attracted particular attention due to their excellent electronic properties, which are strongly determined by the edge of GNRs. For example, a zigzag GNR is metallic[3] (except for ultranarrow ones which are semiconductors[4]), while all thin armchair GNRs are semiconductors with controllable energy gaps.[5,6] So, they are certain candidates for future nanoelectronic devices. There are different types of disorders that can affect the physical and electrical properties of GNRs. The disorders include edge defects, vacancies, potential fluctuations,[7] charge impurities,[8] line and punctual defects,[9] and so on. Until the 1960's, researchers studied just the defects within the constituent graphene layers but did not focus on individual layers.[10,11] Nowadays, due to the development of experimental devices and techniques, the preparation and study of individual layers has become possible.[3,12] It is evident that the theoretical investigations which have been published on two-dimensional honeycomb structures can now be experimentally examined. Still, many theoretical works are being undertaken in order to give a novel suggestion to control and optimize the performance of the electronic conductance by engineering vacancies and structural defects in GNRs. For example, it was shown that due to the localized states appearing near the defect sites, the conductance generally decreases. But the details of this reduction depend on the defect structure, its distance from the edges, and the ribbon width.[13] Further, the studies based on the density functional theory have focused on the influence of different types of line and punctual defects on the structural, electronic, and magnetic properties of graphene sheets and nanoribbons.[9] Moreover, the effect of structural imperfections on transport properties of GNRs has been considered by employing the mean-field Hubbard model along with non-equilibrium Green's function formalism.[7] In the presence of impurities, the conductance strongly depends on the geometrical symmetry and the width of the nanoribbon.[14–17] Finally, some theoretical efforts have been made to model the electronic transport properties of honeycomb nanoribbons.[18,19]

In this paper, we formulate semi-analytically the electronic conductance of a lengthy armchair honeycomb nanoribbon including some vacancies, defects, or impurities by using the Green's function technique within the tight-binding approach. The perturbed or defected part of the GNR is supposed to have a finite length and is located its middle. Therefore, the other parts should be ideal and we can convert their Hamiltonian to the Hamiltonian of some separated chains by using a unitary transformation. The electronic transmission coefficients of some special configurations including vacancies, defects, and electrical impurities are calculated by this model. The paper is organized as follows. In Section 2, we describe the theoretical framework of the model. Section 3 presents the numerical results for some illustrated examples. Section 4 is dedicated to the paper's conclusions.

2. Theoretical model

Here, we present a semi-analytical model to calculate the conductance of a lengthy armchair nanoribbon including some vacancies, defects, or impurities. Consider an ideal honeycomb nanoribbon with infinite length and finite width in which

†Corresponding author. E-mail: mohammad-m@sci.sku.ac.ir

© 2019 Chinese Physical Society and IOP Publishing Ltd

a small part of it (center wire) can be physically different from the other parts (left and right leads). The center wire may include some vacancies, impurities, or even be a single molecule, which is made by omitting some bonds and atoms in this part (see Fig. 3). According to Fig. 1, we label the sites in the center wire by two numbers. The numbers of sites along the length and width are supposed to be N and M, respectively. In this viewpoint, the bonds between the center part and leads play the roles of contacts. The Hamiltonian of the system reads

$$\boldsymbol{H} = \begin{pmatrix} \boldsymbol{H}_{\rm L} & \boldsymbol{H}_{\rm WL} & 0 \\ \boldsymbol{H}_{\rm WL}^{\dagger} & \boldsymbol{H}_{\rm W} & \boldsymbol{H}_{\rm WR} \\ 0 & \boldsymbol{H}_{\rm WR}^{\dagger} & \boldsymbol{H}_{\rm R} \end{pmatrix}, \tag{1}$$

where $\boldsymbol{H}_{\rm L(R)}$, $\boldsymbol{H}_{\rm W}$, and $\boldsymbol{H}_{\rm WL(R)}$ are Hamiltonians of the left (right) lead, center wire, and left (right) contact, respectively. In the tight-binding approach within the first neighbor approximation, $\boldsymbol{H}_{\rm L}$, $\boldsymbol{H}_{\rm W}$, and $\boldsymbol{H}_{\rm R}$ are the block tridiagonal matrices. Their blocks are $\boldsymbol{H}_{i,i}$ and $\boldsymbol{H}_{i,i\pm1}$, where i runs on $-\infty,\ldots,0$ for the left lead, $1,\ldots,N$ for the center wire, and $N+1,\ldots,\infty$ for the right lead. Because of the existence of M atoms in the width, the dimension of each block is $M\times M$. The leads are assumed to have the ideal structures and we suppose that all on-site and hopping energies in them are ε_0 and β, respectively. The hopping energy in the left (right) contact is $\beta_{\rm WL(R)}$. Moreover, we assume that the center wire is connected symmetrically to the leads so that N takes an even number. If one needs the more general formalism, it is easy to come back and redefine different tight-binding parameters. By using these assumptions, we can write the following expressions for the elements in the blocks for the contacts:

$$(\boldsymbol{H}_{\rm WL(R)})_{m,n} = \beta_{\rm WL(R)}\delta_{m,n}, \quad m \text{ is even}, \tag{2}$$

and for the leads:

$$(\boldsymbol{H}_{i,i})_{m,n} = \varepsilon_0\delta_{m,n} + \beta(\delta_{m,n+1} + \delta_{m,n-1}), \tag{3}$$

$$(\boldsymbol{H}_{i,i+1})_{m,n} = \beta\delta_{m,n},$$

$$m \text{ is odd for odd } i, \text{ even for even } i, \tag{4}$$

$$(\boldsymbol{H}_{i,i-1})_{m,n} = \beta\delta_{m,n},$$

$$m \text{ is even for odd } i, \text{ odd for even } i. \tag{5}$$

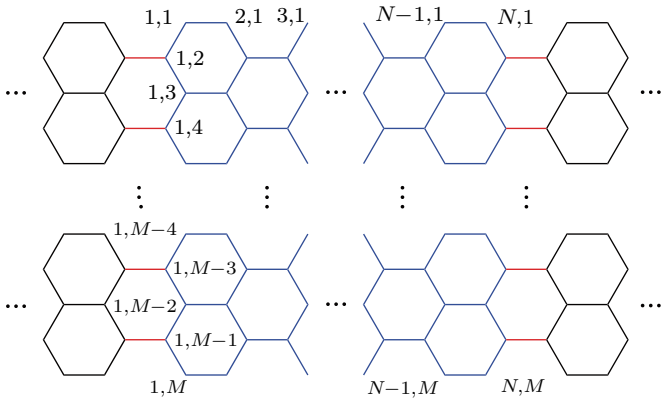


Fig. 1. An infinite ideal honeycomb armchair nanoribbon with a different part at the middle. The blue region is the center part and its sites are labeled by two numbers. This part is connected via some bonds (red lines) to the other parts which will be called as left and right leads (black regions).

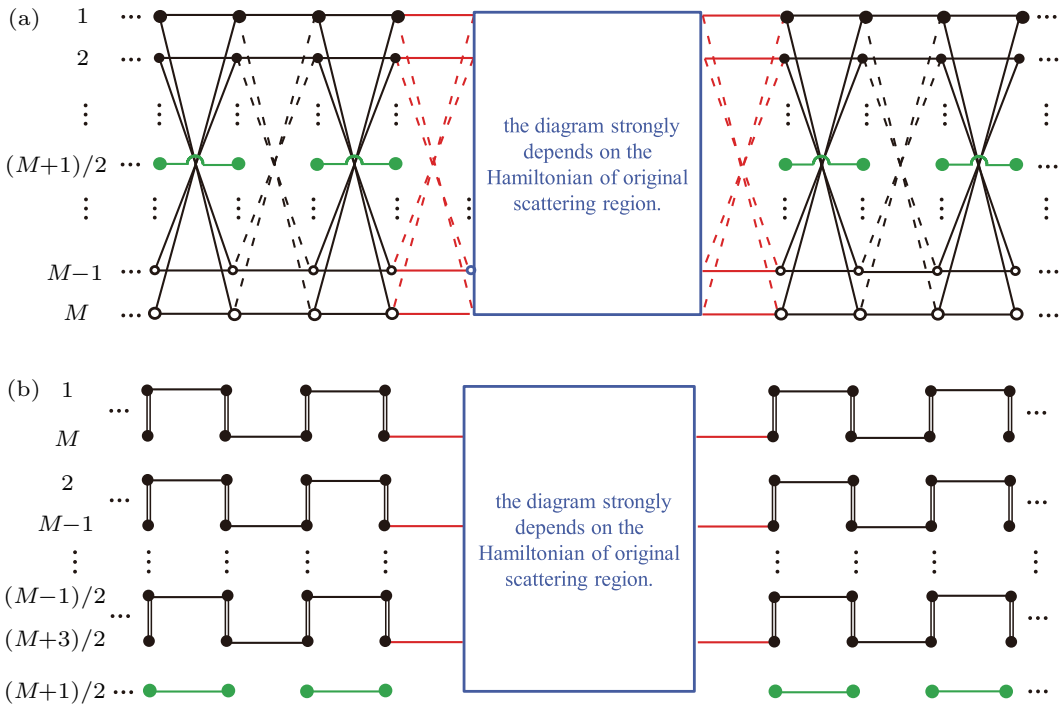


Fig. 2. (a) By applying the transformation matrix U_1 (see Eq. (A1)) on the Hamiltonian of leads presented in Eqs. (3)–(5), $(M-1)/2$ equivalent ladder networks (black) and an independent chain (green) are achieved. (b) By applying the transformation matrix U_2 (see Eq. (A2)), each ladder is converted to an equivalent PA-like chain with on-sites and hopping terms which are given by Eqs. (A6) and (A7).

For an ideal nanoribbon, the Hamiltonian of the center wire is exactly the same as the above Hamiltonian. However, when the vacancies, defects, or impurities exist, the corresponding tight-binding parameter should be set to zero or redefined. In Appendix A, we introduce two unitary matrices which transform the Hamiltonian of the ideal parts of the armchair honeycomb nanoribbon to the Hamiltonian of some equivalent polyacetylene-like (PA-like) chains. In Figs. 2(a) and 2(b), we present the equivalent tight-binding structures earning by applying the first and second transformations, respectively. In fact, the transformed Hamiltonian of the leads is simplified to the Hamiltonians of the $(M-1)/2$ different semi-infinite PA-like chains with alternative $2\beta\left|\cos\left(n\pi/(M+1)\right)\right|$ and β hopping terms (see Eqs. (A6) and (A7) as well as Fig. 2(b)). Now, the inverse of the transformed Green's function matrix of the center part in the presence of these chains reads

$$\boldsymbol{G}_{\mathrm{W}}^{-1} = \begin{pmatrix} \varepsilon\boldsymbol{I}-\tilde{\boldsymbol{H}}_{1,1}-\tilde{\boldsymbol{\Sigma}}_{\mathrm{L}} & -\tilde{\boldsymbol{H}}_{1,2} & \cdots & \boldsymbol{0} \\ -\tilde{\boldsymbol{H}}_{2,1} & \varepsilon\boldsymbol{I}-\tilde{\boldsymbol{H}}_{2,2} & \cdots & \boldsymbol{0} \\ \vdots & \vdots & \ddots & \vdots \\ \boldsymbol{0} & \boldsymbol{0} & \cdots & \varepsilon\boldsymbol{I}-\tilde{\boldsymbol{H}}_{N,N}-\tilde{\boldsymbol{\Sigma}}_{\mathrm{R}} \end{pmatrix}, \quad (6)$$

where ε is the electron energy, $\boldsymbol{I}$ is $M\times M$ identity matrix, and $\tilde{\boldsymbol{\Sigma}}_{\mathrm{L(R)}}$ is the left (right) transformed self-energy matrix containing self-energy functions of the center part in the presence of the aforementioned PA-like chains. Here, $\tilde{\boldsymbol{H}}_{i,i}$ and $\tilde{\boldsymbol{H}}_{i,i\pm1}$ are the transformed Hamiltonian matrices corresponding to $\boldsymbol{H}_{i,i}$ and $\boldsymbol{H}_{i,i\pm1}$ belonging to the center part in which i runs from 1 to N. The matrix elements of $\tilde{\boldsymbol{\Sigma}}_{\mathrm{L(R)}}$ can be easily calculated by the following formula:[20]

$$\begin{aligned}(\tilde{\boldsymbol{\Sigma}}_{\mathrm{L(R)}})_{m,n} &= \tilde{\Sigma}^{(n)}_{\mathrm{L(R)}} \\ &= \frac{\beta^2_{\mathrm{WL(R)}}(\varepsilon-\varepsilon_0)}{(\varepsilon-\varepsilon_0)^2-4\beta^2\cos^2\dfrac{n\pi}{M+1}-2\beta^2\left|\cos\dfrac{n\pi}{M+1}\right|\mathrm{e}^{-\mathrm{i}\theta_n}}\delta_{m,n}, \\ &\text{for } n>\frac{M-1}{2};\ (\tilde{\boldsymbol{\Sigma}}_{\mathrm{L(R)}})_{m,n}=0, \quad \text{otherwise}, \end{aligned} \quad (7)$$

where

$$\cos\theta_n = \frac{(\varepsilon-\varepsilon_0)^2-\beta^2\left(2\cos\dfrac{2n\pi}{M+1}+3\right)}{4\beta^2\cos^2\dfrac{n\pi}{M+1}}. \quad (8)$$

Therefore, the formalism provides the electronic transmission coefficient of the system as

$$T(\varepsilon) = \mathrm{tr}\left(\boldsymbol{\Gamma}_{\mathrm{L}}\boldsymbol{G}^{\dagger}_{\mathrm{W}}\boldsymbol{\Gamma}_{\mathrm{R}}\boldsymbol{G}_{\mathrm{W}}\right), \quad (9)$$

where $\boldsymbol{\Gamma}_{\mathrm{L(R)}} = -2\mathrm{Im}\,\tilde{\boldsymbol{\Sigma}}_{\mathrm{L(R)}}$. There are some configurations in which the transmission coefficient of the system is the sum of $(M-1)/2$ transmission coefficients of independent chains

$$T(\varepsilon) = \sum_{n=1}^{(M-1)/2} T_n(\varepsilon). \quad (10)$$

In this case, at each unit cell of the center wire, all the atoms, as well as all the bonds, should be identical. When their tight-binding parameters take the same values even in different unit cells, one can obtain a useful fully analytic formalism. The example is an ideal infinite nanoribbon including two linear transverse defects. That is an ideal nanoribbon connected to two same ideal nanoribbons via weaker or stronger bonds ($\beta_{\mathrm{WL(R)}}\neq\beta$). For this problem, by using the formalism introduced in Ref. [21], we obtain

$$T_n(\varepsilon) = \frac{16\,\mathrm{Im}\,\tilde{\Sigma}^{(n)}_{\mathrm{L}}\,\mathrm{Im}\,\tilde{\Sigma}^{(n)}_{\mathrm{R}}\cos^2\dfrac{n\pi}{M+1}}{\beta^2\left|\tilde{D}^{(n)}_{N}(\varepsilon,\tilde{\Sigma}^{(n)}_{\mathrm{L}},\tilde{\Sigma}^{(n)}_{\mathrm{R}})\right|^2}, \quad (11)$$

where

$$\begin{aligned}&\beta^2\tilde{D}^{(n)}_{N}(\varepsilon,\tilde{\Sigma}^{(n)}_{\mathrm{L}},\tilde{\Sigma}^{(n)}_{\mathrm{R}}) \\ &= \Big((\varepsilon-\varepsilon_0)^2-(\tilde{\Sigma}^{(n)}_{\mathrm{L}}+\tilde{\Sigma}^{(n)}_{\mathrm{R}})(\varepsilon-\varepsilon_0) \\ &\quad +\tilde{\Sigma}^{(n)}_{\mathrm{L}}\tilde{\Sigma}^{(n)}_{\mathrm{R}}-4\beta^2\cos^2\frac{n\pi}{M+1}\Big)D^{(n)}_{N-1}(\varepsilon) \\ &\quad +2(\tilde{\Sigma}^{(n)}_{\mathrm{L}}\tilde{\Sigma}^{(n)}_{\mathrm{R}}-\beta^2)\left|\cos\frac{n\pi}{M+1}\right|D^{(n)}_{N-3}(\varepsilon), \end{aligned} \quad (12)$$

with

$$D^{(n)}_{l} = \frac{\sin((l+1/2)\theta_n)}{\sin(\theta_n/2)}, \quad l=N-1,N-3, \quad (13)$$

in which θ_n is determined by Eq. (8).

3. Numerical results

Consider an ideal lengthy armchair honeycomb nanoribbon as shown in Fig. 1; and let a small part of it be different in existence of defects, vacancies, or impurities. Figure 3 shows some examples of these defective nanoribbons that we consider in this paper. They are the selected configurations that the presented formalism in the previous section can easily apply on them. Since all the on-site energies, as well as all the hopping terms, are the same in the whole of each chosen structure, then without loss of generality, we can choose the arbitrary values for these energies. To perform numerical calculations, we fix the width of the nanoribbon at $M=9$ and we set all on-site and hopping energies equal to zero and 1 eV, respectively. The electronic transmission coefficients of these configurations as the functions of energy are plotted in Fig. 4. Since the transmission curves are symmetric with respect to zero energy, we only present them for positive energies. For an ideal nanoribbon, the transmission curve is a step-function and due to the overlapping of four $((M-1)/2)$ conductance modes, it gets the maximum value of 4. In the presence of defects, the translational symmetry of the nanoribbon network is eliminated and obvious changes are created in the transmission curve especially moving out of its stair shape. In general, an ideal armchair nanoribbon has the semi-metallic behavior due to the existence of a small gap around the zero energy. The results corresponding to Figs. 3(a) and 3(b) plotted

in Fig. 4 show that in the presence of one (Fig. 3(a)) or two (Fig. 3(b)) vacancies, the energy gap increases with respect to that of the ideal structure. Moreover, by increasing the number of neighbor vacancies, the transmission coefficient of the system decreases and takes a smoother shape with respect to energy. If the geometry of the center wire is different from the ideal nanoribbon geometry, then the conductance curve gets out from the step form. In fact, the electron scatters by the electric potential of the defects. Numerical investigations for coherent transport of structures depicted Fig. 3(a) can be found in Refs. [22]–[25].

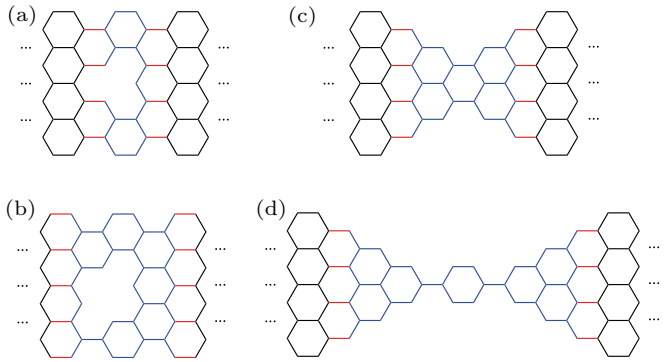


Fig. 3. Some examples studied in this paper for a lengthy armchair honeycomb nanoribbon with a defective part at the middle.

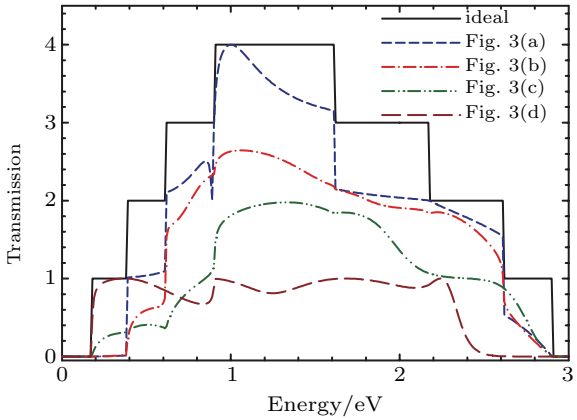


Fig. 4. Transmission coefficient of a lengthy nanoribbon (with $M = 9$) containing some defects in a small part of it. The configurations are shown in Fig. 3. All the on-site and hopping energies of the system are taken as $\varepsilon_0 = 0$ and $\beta = 1$ eV, respectively.

In Figs. 3(c) and 3(d), some bonds and atoms are omitted in a part of the nanoribbon so that its width smoothly reduces to one hexagonal ring molecule. They can be interpreted as two possible cases in which a hexagonal molecule is connected to two semi-infinite nanoribbons symmetrically. In this viewpoint, we expect that the electrical conductivity depends on the electronic properties of the molecule. It is also highly sensitive to the structures and geometry of the leads and contacts. In fact, the coupling between the conductors and the molecule causes the overlapping of their electronic states and leads to the expansion of molecular electronic orbits. A study for electronic transport properties of a zigzag structure similar to that in Fig. 3(d) has been performed in Ref. [26]. In Fig. 4, it can be seen that the conductivity for these cases (Figs. 3(c) and 3(d)) is significantly smaller than the ideal nanoribbon conductivity. Here, the participating conductance channels decrease due to the dismissal of several connection bonds. Therefore, it is acceptable that the decrease in the conductance is more for the case of Fig. 3(d) with respect to the case of Fig. 3(c). Considering a molecule as the central system, we actually have edge roughness in a small part of the nanoribbon. It is obvious from Fig. 4 that the higher edge roughness causes the lower conductivity. Also, the transmission coefficient is considerably reduced at energies near the Fermi energy.

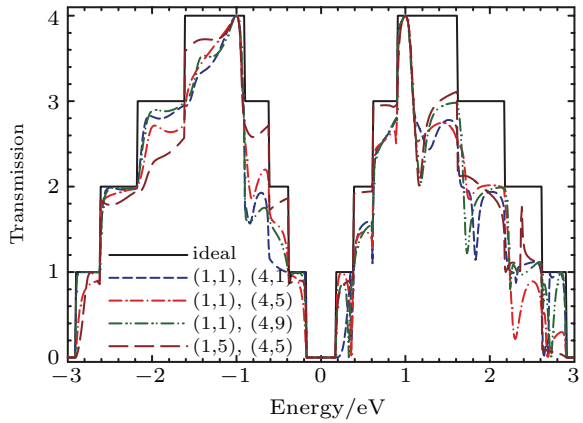


Fig. 5. Transmission coefficient of a lengthy nanoribbon ($M = 9$) with two impurities in the central part. The locations of the impurities are distinguished by two integer numbers (see Fig. 1 for a better understanding of the coordinates). Here, the on-site energies of the impurities are set to 1.5 eV. The other on-site and hopping energies of the system are taken as $\varepsilon_0 = 0$ and $\beta = 1$ eV, respectively.

Electronic properties of doped nanoribbons are very different from those of pure ones. The presence of impurities makes resonant backscattering whose features depend on the width of the nanoribbon and the position of the impurities.[14] By the proposed model in this paper, we are able to investigate semi-analytically the conductance of an ideal lengthy armchair nanoribbon in the presence of some impurities which are distributed at a finite part of it. In Figs. 5 and 6, we plot the transmission coefficient of an armchair nanoribbon with width $M = 9$ including two impurities as a function of energy for some different positions of the impurities. For Fig. 5, we take the on-site energy of each impurity identical to 1.5 eV, while for Fig. 6 they are chosen as ± 1.5 eV. The different curves correspond to different positions of the two impurities which are represented with their coordinates as defined in Fig. 1. Among all possible sites, four and six different arrangements for the impurities are shown in Figs. 5 and 6, respectively. In the case that the impurities are located at $(1,5)$ and $(4,5)$, a Fano resonance, a sudden decrease and increase of transmission coefficient, appears at energy $\varepsilon = 2.36$ eV. It happens due to the existence of different physical paths for the passing electron wave function.[8] The existence of conducting valleys especially in the boundaries of the conduction channels is due to the destructive interference of the electronic wave functions.

When the impurities are located near the edges of the nanoribbon, the conductance is affected more with respect to the case that they lie far away from the edges. In fact, the electrons do not easily move through imperfections because of electronic localization at the edges.

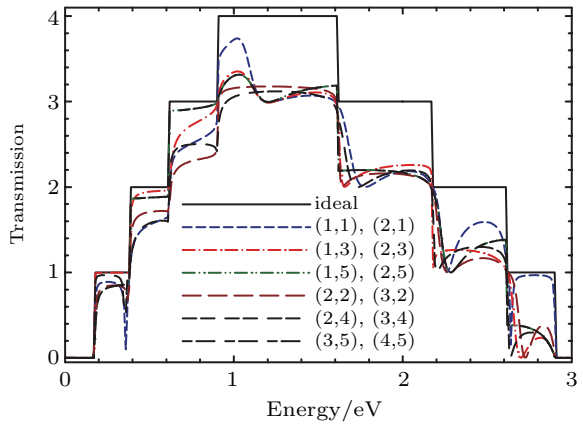


Fig. 6. Transmission coefficient of a lengthy nanoribbon with $M = 9$. There are two impurities in the form of an electric dipole (with on-site energies ± 1.5 eV) in a small part of the nanoribbon (central wire). The locations of the impurities are distinguished by two integer numbers (see Fig. 1 for better understanding of the coordinates). The other on-site and hopping energies of the system are taken as $\varepsilon_0 = 0$ and $\beta = 1$ eV, respectively.

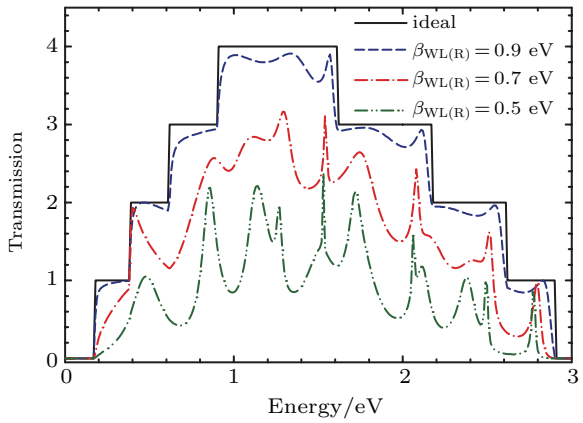


Fig. 7. Transmission coefficient of a lengthy nanoribbon with $M = 9$ for some different values $\beta_{WL(R)}$. The central system (with $N = 6$) and the connected nanoribbons are supposed to be ideal. Here, we take $\beta = 1$ eV and $\varepsilon_0 = 0$.

Now, we examine the fully analytically formalism based on Eqs. (10)–(13) by a simple example. In this example, the contact bonds of the lengthy armchair nanoribbon introduced in Fig. 1 are different from others (linear transverse defects). In fact, the center part and leads are the same and changes are applied only to the hopping energies of the contact bonds. Figure 7 displays the transmission coefficient of the structure with $M = 9$ and $N = 6$ as a function of energy for some different values of $\beta_{WL(R)}$. We see that the transmission coefficient decreases and its valleys and peaks become deeper and sharper, respectively, by reducing the hopping energy in the connection bonds. The decreasing of $\beta_{WL(R)}$ makes the conductance peaks sharper. The reason refers to the fact that the quasi-energies of the middle parts become well-defined and the electron relaxation time in them are longer.

4. Conclusion

We introduce a semi-analytical model to study the electronic conductance of a lengthy armchair nanoribbon, a part of which is different due to the existence of vacancies, defects, or impurities. We use Green's function technique within the tight-binding approach and linear response theory. We have also formulated fully analytically the electronic conductance of an ideal infinite armchair nanoribbon with arbitrary width. It is shown that the Hamiltonian of a semi-infinite ideal armchair nanoribbon can be converted to the Hamiltonian of some PA-like chains with alternative hopping terms. Therefore, the fully analytical formulas for self-energies have been obtained and the transmission coefficient can be calculated by inverting a small matrix with the size of the perturbed part of the nanoribbon. This introduces a fast calculating semi-analytical method which is suitable for any arbitrary size of armchair nanoribbons. In addition to ideal nanoribbons, in some symmetric configurations, the transmission coefficient is easily obtained with the summation of the transmission coefficients of some independent chains with fully analytical tools.

To show the ability of the model, we have calculated the electronic transmission coefficient for some illustrated examples including different configurations in Fig. 3 as well as a nanoribbon including one or two impurities. In general, the presence of imperfections causes the reduction of the electronic conductance and variation in the value of the central energy gap. Indeed, one may design a molecular electronic device by removing some bonds and atoms or impurity injections on a small part of the armchair nanoribbon.

Appendix A: unitary transformation

Here, we introduce the following unitary transformation matrices in order to convert the Hamiltonian of an ideal armchair honeycomb nanoribbon to the Hamiltonian of some PA-like chains:

$$(U_1)_{m,n} = \sqrt{\frac{2}{M+1}} \sin \frac{\pi mn}{M+1}, \tag{A1}$$

$$U_2 = \frac{1}{\sqrt{2}} \begin{pmatrix} & & 0 & & \\ & \boldsymbol{I} & \vdots & \boldsymbol{J} & \\ 0 & \cdots & \sqrt{2} & \cdots & 0 \\ & \boldsymbol{J} & \vdots & -\boldsymbol{I} & \\ & & 0 & & \end{pmatrix}, \tag{A2}$$

where $\boldsymbol{I}$ and $\boldsymbol{J}$ are identity and backward-identity matrices of size $(M-1)/2$, respectively. By applying these transformations to the Hamiltonians introduced in Eqs. (3)–(5), we have

$$(\boldsymbol{U}_1^{\dagger} \boldsymbol{H}_{i,i} \boldsymbol{U}_1)_{m,n} = \left(\varepsilon_0 + 2\beta \cos \frac{n\pi}{M+1}\right) \delta_{m,n}, \tag{A3}$$

$$\boldsymbol{U}_1^{\dagger}\boldsymbol{H}_{i,i\pm1}\boldsymbol{U}_1 = \frac{\beta}{2}\begin{pmatrix} & & 0 & & \\ & \boldsymbol{I} & \vdots & \boldsymbol{J} & \\ 0 & \cdots & 2 & \cdots & 0 \\ & \boldsymbol{J} & \vdots & \boldsymbol{I} & \\ & & 0 & & \end{pmatrix},$$

$$+ \text{ for odd } i, - \text{ for even } i; \tag{A4}$$

$$\boldsymbol{U}_1^{\dagger}\boldsymbol{H}_{i,i\pm1}\boldsymbol{U}_1 = \frac{\beta}{2}\begin{pmatrix} & & 0 & & \\ & \boldsymbol{I} & \vdots & -\boldsymbol{J} & \\ 0 & \cdots & 0 & \cdots & 0 \\ & -\boldsymbol{J} & \vdots & \boldsymbol{I} & \\ & & 0 & & \end{pmatrix},$$

$$+\text{for even } i, - \text{ for odd } i; \tag{A5}$$

$$(\boldsymbol{U}_2^{\dagger}\boldsymbol{U}_1^{\dagger}\boldsymbol{H}_{i,i}\boldsymbol{U}_1\boldsymbol{U}_2)_{m,n} = \varepsilon_0\delta_{m,n} + 2\beta\left|\cos\frac{n\pi}{M+1}\right|\delta_{m,M+1-n}, \tag{A6}$$

$$(\boldsymbol{U}_2^{\dagger}\boldsymbol{U}_1^{\dagger}\boldsymbol{H}_{i,i\pm1}\boldsymbol{U}_1\boldsymbol{U}_2)_{m,n} = \beta\delta_{m,n} \begin{cases} +\text{for odd } i, - \text{ for even } i, & n \le \dfrac{M+1}{2}, \\ -\text{for odd } i, + \text{ for even } i, & n > \dfrac{M+1}{2}. \end{cases} \tag{A7}$$

Also, the transformed Hamiltonian for contacts in Eq. (2) is the same as the above equation with $\beta_{\mathrm{WL(R)}}$ instead of β under the lower condition.

References

[1] Torres L E F F, Roche S and Charlier J C 2014 *Introduction to Graphene-Based Nanomaterials* (Cambridge: Cambridge University Press)

[2] Katsnelson M I 2012 Graphene: Carbon in Two Dimensions (Cambridge: Cambridge University Press)

[3] Novoselov K, Geim A and Morozov S 2004 *Science* **306** 666

[4] Li X, Wang X, Zhang L, Lee S and Dai H 2008 *Science* **319** 1229

[5] Cai J, Ruffieux P, Jaafar R, Bieri M, Braun T, Blankenburg S, Muoth M, Seitsonen A P, Saleh M, Feng X, Müllen K and Fasel R 2010 *Nature* **466** 470

[6] Blankenburg S, Cai J, Ruffieux P, Jaafar R, Passerone D, Feng X, Müllen K, Fasel R and Pignedoli C A 2012 *ACS Nano* **6** 2020

[7] Djavid N, Khaliji K, Tabatabaei S M and Pourfath M 2014 *IEEE T. Electron Dev.* **61** 23

[8] Chauhan S S, Srivastava P and Shrivastava A K 2014 *Appl. Nanosci.* **4** 461

[9] Guerra T, Azevedo S and Machado M 2016 *Eur. Phys. J. B* **89** 58

[10] Thrower P A and Mayer R M 1987 *Phys. Status. Solidi. (a)* **47** 11

[11] Thrower P A 1964 *Brit. J. Appl. Phys.* **15** 1153

[12] Koch M, Li Z, Nacci C, Kumagai T, Franco I and Grill L 2018 *Phys. Rev. Lett.* **121** 047701

[13] Gorjizadeh N, Farajian A A and Kawazoe Y 2008 *Nanotech. Let.* **20** 015201

[14] Biel B, Blase X, Triozon F and Roche S 2009 *Phys. Rev. Lett.* **102** 096803

[15] Zheng X H, Rungger I, Zeng Z and Sanvito S 2009 *Phys. Rev. B* **80** 235426

[16] Smith C W, Katoch J and Ishigami M 2013 *Appl. Phys. Lett.* **102** 133502

[17] Rabani H, Mardaani M and Mazloom Shahraki A 2013 *Superlattice. Microst.* **59** 106

[18] Sharmaa B L 2018 *Eur. Phys. J. B* **91** 84

[19] Stegmann T, Franco-Villafañe J A, Kuhl U, Mortessagne F and Seligman T H 2017 *Phys. Rev. B* **95** 035413

[20] Mardaani M and Rabani H 2013 *J. Magn. Magn. Mater.* **331** 28

[21] Mardaani M, Rabani H and Esmaeili A 2011 *Solid State Commun.* **151** 928

[22] Xiong Y J and Kong X L 2010 *Physica B* **405** 1690

[23] Lehmann T, Ryndyk D A and Cuniberti G 2013 *Phys. Rev. B* **88** 125420

[24] Ihnatsenka S and Kirczenow G 2009 *Phys. Rev. B* **80** 201407R

[25] Haskins J, Kýnacý A, Sevik C, Sevinc-li H, Cuniberti G and Çağın T 2011 *ACS Nano* **5** 3779

[26] Simchi H, Esmaeilzadeh M and Saani M H 2012 *Phys. Status Solidi B* **249** 1735